

Development of magnetosomes-based biosensor for the detection of *Listeria monocytogenes* from food sample

 ISSN 1751-8741
 Received on 13th April 2020
 Revised 24th August 2020
 Accepted on 15th September 2020
 E-First on 2nd November 2020
 doi: 10.1049/iet-nbt.2020.0091
 www.ietdl.org

 Sumana Sannigrahi¹, Shiva Kumar Arumugasamy², Jayaraman Mathiyarasu², Krishnamurthy

 Suthindhiran¹ ✉

¹Marine Biotechnology and Bioproducts Lab, School of Biosciences and Technology, VIT-Vellore, 632014 Tamil Nadu, India

²Electrodics and Electrocatalysis Division, CSIR – Central Electrochemical Research Institute, Karaikudi 630003, Tamil Nadu, India

✉ E-mail: ksuthindhiran@vit.ac.in

Abstract: Listeriosis through contaminated food is one of the leading causes of premature deaths in pregnant women and new born babies. Here, the authors have developed a magnetosomes-based biosensor for the rapid, sensitive, specific and cost-effective detection of *Listeria monocytogenes* from food sample. Magnetosomes were extracted from *Magnetospirillum sp.* RJS1 and then directly bound to anti-Listeriolysin antibody (0.25–1 µg/ml), confirmed in spectroscopy. Listeriolysin (LLO) protein (0.01–7 µg/ml) was optimised in enzyme-linked immunosorbent assay. Magnetosomes was conjugated with LLO antibody (0.25 µg/ml) in optimum concentration to detect LLO protein (0.01 µg/ml). Magnetosomes–LLO antibody complex was 25% cost effective. The magnetosomes–LLO antibody complex was directly stabilised on screen printed electrode using external magnet. The significant increase in resistance (R_{CT} value) on the electrode surface with increase in concentration of LLO protein was confirmed in impedance spectroscopy. The *L. monocytogenes* contaminated milk and water sample were processed and extracted LLO protein was detected in the biosensor. The specificity of the biosensor was confirmed in cross-reactivity assay with other food pathogens. The detection limit of 10^1 CfU/ml in both water and milk sample manifests the sensitive nature of the biosensor. The capture efficiency and field emission scanning electron microscopy confirmed positive interaction of *Listeria* cells with magnetosomes–antibody complex.

1 Introduction

Listeria monocytogenes are the most prevailing food pathogen with huge mortality rates causing life threatening gastroenteritis, meningo-encephalitis and sepsis [1, 2]. The major population affected by Listeriosis consists of immune compromised patients of HIV, cancer, diabetes, pregnant or lactating women's and new born babies [3]. The prime sources of *Listeria* infection are fish and seafood products (6%), ready to eat salads (4.2%), meat-based products (1.8%), dairy (0.9%), fruit and vegetables (0.6%) [4, 5]. World Health Organization (WHO) has considered *L. monocytogenes* as one of the most lethal pathogens as it can withstand severe pH, high salt concentration and low-temperature conditions reporting 1 million per year cases in South-East Asian countries [6]. India being one of the largest producers of fish has reported the presence of *L. monocytogenes* in seafood's and fishes available in Tuticorin region, Kerala and Kashmir [7–10]. Moreover, multidrug-resistant strains of *L. monocytogenes* have been also reported in raw milk from major areas of Rajasthan [11], cattle milk in Odisha [12] and sacred milk offered to devotees in Tiruchirappalli [13].

The initial internalisation of *L. monocytogenes* in the mammalian cells occurs through the surface proteins internalin (InlA and InlB) [14]. However, the pore-forming protein listeriolysin O (LLO) is the primary virulence factor in *L. monocytogenes* as it helps the bacteria to escape phagolysosome and further multiplication in host cytoplasm [14, 15]. The recent studies have also stated the importance of LLO protein as an extracellular signalling molecule during the infection and its role in initial entry in host cells [16, 17]. The complicated symptoms formed during the listeriosis causes delay in the diagnosis resulting in more mortality cases compared to other food pathogens [17, 18]. Besides, the conventional methods are inefficient, time consuming and involve multistep protocols [19, 20].

Antibody-based biosensors are widely known for its simple, sensitive and fast detection of food pathogens [21–24]. Most of the

studies involve surface immobilisation of the antibodies on the electrode through physical adsorption, covalent attachment and cross-linker [25]. However, the stability and free functioning of antibodies on the electrode surface are often compromised during the process [26]. Nanoparticle, on the other hand, provides large surface area for biomolecule interaction thereby enhancing the charge transfer capacity and sensitivity of biosensors [27–29]. Further, magnetic nanoparticles can accurately place the biomolecules on the electrode surface, hence significantly reducing the time [30, 31]. Despite the numerous applications of magnetic nanoparticles in the biosensor, challenges in biocompatibility due to use of linker molecules and lack of uniformity in size of nanoparticles are major problem in developing biosensor [32].

Alternatively, magnetosomes are biologically synthesised nanoparticle with uniform particle shape, narrow size distribution, ferromagnetic domain and high magnetic susceptibility to manifest its importance over conventional synthetic nanoparticles [33, 34]. Magnetosomes are composed of Fe_3O_4 , generally synthesised in magnetotactic bacteria through biomineralisation process [35]. The magnetosomes contains an outer lipid bilayer membrane which is mainly formed of phosphatidylserine and phosphatidylethanolamine that provides amine group to the magnetosomes surface [36]. The natural presence of lipid bilayer membrane acts as a signal transducer for antibody–antigen reaction [37].

The current study focuses on developing a biosensor where magnetosomes are directly conjugated with anti-LLO antibody. The active LLO protein and the cells of *L. monocytogenes* act as an analyte to be detected in the developed biosensor.

2 Materials and methodology

2.1 Chemicals and antibodies

The chemicals used in this study were purchased from HiMedia Laboratories, India. The primary antibody (anti-LLO antibody, ab200538), secondary antibody (goat anti-rabbit IgG) labelled with

horseradish peroxidase (HRP) (ab205718) and the recombinant LLO protein (ab83345) were purchased from Abcam, India. (2, 2' azino-(di-3-ethylbenzthiozoline sulfonic acid) ABTS was purchased from SRL Limited, India. Screen printed carbon electrode (SPCE) RRPE1002C was purchased from Pine Research Instrumentation, Durham, USA. Microbial culture stocks of *L. monocytogenes* (MTCC- 657), *Salmonella typhimurium* (MTCC 98), *Escherichia coli* (MTCC 1687) and *Staphylococcus aureus* (MTCC 1144) were purchased from Microbial Type Culture Collection and Gene Bank (MTCC), India.

2.2 Culturing of bacteria

The sediment samples were collected from Pulicat lagoon in South east coast of India. CARD-FISH method was implemented on sediment samples to determine the presence of MTB. Then, the MTB was isolated through capillary racetrack method, purification and gradient cultivation. The 16S rRNA gene sequence analysis showed that the isolate belongs to Alphaproteobacteria with 99% similarity with MSR-1 [38]. The test organism *Magnetospirillum* sp. RJS1 [38] was cultured in *Magnetospirillum* growth media through Hungate anaerobic technique [39]. The growth of the culture and production of magnetosomes was monitored at regular interval by placing the culture bottle on a magnetic stirrer against a continuous light source [40].

2.3 Magnetosomes extraction and its analytical characterisation

The *Magnetospirillum* sp. RJS1 culture was collected and centrifuged (Refrigerated Centrifuge LI-HRC-16K, Lark Innovative Fine Teknowledge, India) at $8000 \times g$ for 10 min. The pellet obtained was resuspended in Tris-HCL and sonicated (VCX-130W-220VAC-VIBRA-CELL SYSTEM, Sonics & Materials, Inc., USA) at 35 kHz for 2 h. The magnetosomes were then separated out from the cell debris using an external magnetic field [40]. Magnetosomes were lyophilised (Lark, Penguin Classic Plus, India) and characterised through high-resolution transmission electron microscopy (HR-TEM, JEOL JEM2100, Japan operating at 200kv), field emission scanning electron microscopy (FESEM, Zeiss EV018, Germany operating at 10kv) and energy-dispersive X-ray spectroscopy (EDS). Magnetosomes were uniformly dispersed in distilled water and drop casted on slides. The slides were dried for overnight at room temperature and viewed under FESEM. HR-TEM analysis was done by directly drop casting the dispersed magnetosomes on the copper grid and viewed under the microscope.

2.4 Preparation of magnetosomes-anti-LLO antibody complex

The protocol for functionalisation of magnetosomes with anti-LLO antibody was modified and adapted from Woo *et al.* [41]. Magnetosomes (1 mg, 2 mg) were uniformly dispersed through sonication in 1 ml phosphate buffer saline (PBS). Then, 100 μ l of anti-LLO antibody (1 μ g/ml) was added to 900 μ l of dispersed magnetosomes (1, 2 mg/ml) solution and incubated at 4°C for 24 h. The magnetosomes-anti-LLO antibody complex were concentrated using the external magnetic field. The conjugates of magnetosomes-anti-LLO antibody were briefly washed with 1% bovine serum albumin prepared in PBS for 10–12 times to remove the free antibodies. The absorbance of conjugates, free antibodies and free magnetosomes were recorded at 630 nm in 96-plate reader (LIMR96, Lark Innovative Fine Teknowledge, India) to determine the conjugation of magnetosomes with anti-LLO antibody. Similarly, conjugates of magnetosomes (1, 2 mg/ml) with other concentrations of anti-LLO antibody (0.83–0.25 μ g/ml) were also prepared.

Electrochemical impedance spectroscopy (EIS) was performed to determine the magnetosomes-anti-LLO antibody conjugation through the charge transfer in electrode surface [42]. A series of screen-printed carbon electrodes that consists of a carbon working electrode, a carbon counter electrode and a silver reference electrode were chosen for this study. The SPCE's were pre-treated

with 0.1 M Na_2CO_3 , at 1.2 V to activate the electrode surface. Briefly, 10 μ l of anti-LLO antibody (1 μ g/ml) was cast on the working electrode and incubated at 37°C for 30 min. After the incubation, the electrode was rinsed with PBS buffer for 30 s and then twice in deionised water. EIS measurement was done in 10 mM PBS (pH 7.4) containing 1 mM $\text{K}_4[\text{Fe}(\text{CN})_6]$, 1 mM $\text{K}_3[\text{Fe}(\text{CN})_6]$ and 0.1 M KCl. The experiment was performed in an open circuit model with 0.13 V potential. The impedance measurements were recorded against imaginary versus real impedance from 0.1 Hz to 100 kHz, with amplitude of 10 mV. ZVIEW software was used to generate a fitting spectrum from the data obtained during the experiment. Similarly, the impedance response for various concentrations (0.25–1 μ g/ml) of anti-LLO antibody was measured. For magnetosomes and magnetosomes-anti-LLO antibody conjugate, a bar magnet was placed below the SPCE prior to the experiment and impedance response was obtained.

2.5 Methods for screening active LLO protein

2.5.1 Binding of LLO with magnetosomes-anti-LLO antibody complex: A stock solution of LLO (0.1 μ g/ml) was prepared in carbonate-bicarbonate buffer stock (pH 9.2). Briefly, 100 μ l of LLO was loaded on the 96-well plate and incubated at 4°C overnight for LLO attachment on the plate. After the incubation, the wells were washed with PBS-tween 20 (PBST) for three times to remove unbound LLO and incubated at room temperature for 5 min. The process was repeated again and then 100 μ l of magnetosomes (1 or 2 mg/ml)-anti-LLO antibody (0.25–1 μ g/ml) complex was loaded to the washed wells. A bar magnet was placed below the plate to aggregate the magnetosomes-antibody-antigen complex and incubated at 37°C for 60 min. The plate was washed with PBST for three times and absorbance was taken at 630 nm. The absorbance of magnetosomes-anti-LLO antibody complex without LLO and absorbance of magnetosomes without anti-LLO antibody and LLO was also taken.

2.5.2 Magnetosomes-based colorimetric assay to detect LLO: Enzyme-linked immunosorbent assay (ELISA) was performed using magnetosomes (1 or 2 mg/ml)-anti-LLO antibody and secondary antibody to detect the LLO. A stock solution of 0.1 μ g/ml LLO (100 μ l) was incubated in 96-well plate at 4°C for overnight. Next, the LLO coated wells were washed PBST and 100 μ l of each stock solution for magnetosomes (1, 2 mg/ml)-anti-LLO antibody (0.25–1 μ g/ml) complex were further incubated at 37°C for 60 min. After the incubation, a neodymium bar magnet was placed beneath the titre plate and the wells were washed thrice with PBST. A control without magnetosomes, i.e. anti-LLO antibody (0.25–1 μ g/ml) was also maintained. Next, 100 μ l of secondary antibody-HRP (1 μ g/ml) was added to the washed wells. Incubation and washing step were followed similar to primary antibody and then, 100 μ l of ABTS substrate was added to the washed wells. After 30 min incubation, absorbance was measured at 405 nm in a plate reader.

Further, the minimum concentration of LLO was detected in ELISA. LLO in various concentrations (0.01–7 μ g/ml) was coated (100 μ l) on the wells. Washing step was performed and further 100 μ l of magnetosomes (1, 2 mg/ml)-anti-LLO antibody (0.25 μ g/ml) complex and secondary antibody HRP (1 μ g/ml) was subsequently loaded. Absorbance was measured at 405 nm after adding the ABTS substrate.

2.5.3 Fabrication of SPCE to detect LLO: The SPCE's were fabricated with the most optimum concentration of magnetosomes (2 mg/ml)-anti-LLO antibody (0.5 μ g/ml) complex to detect LLO in EIS. The complex was stabilised on the electrode surface using an external magnet. Next, 10 μ l of LLO at various concentrations (0.01–7 μ g/ml) was applied to the fabricated electrode and incubated at 37°C for 60 min. After the incubation, the electrode was rinsed with PBS and deionised water. EIS measurements were carried out in PARSTAT (Princeton Applied Research) electrochemical workstation. A control set (anti-LLO antibody without magnetosomes) was also studied to detect the LLO.

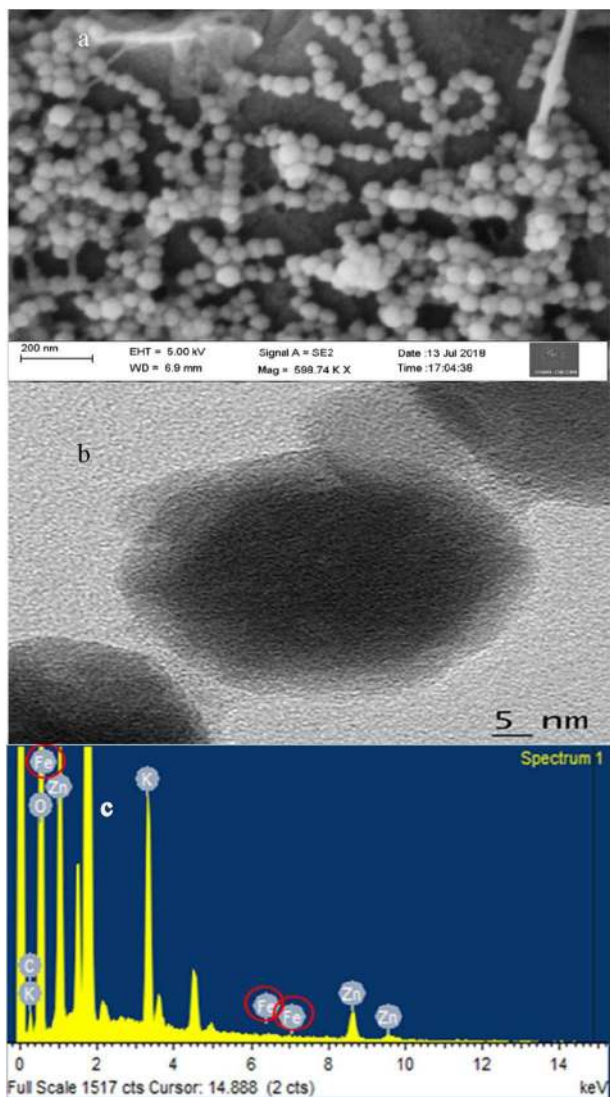


Fig. 1 Characterisation of magnetosomes
(a) FESEM image confirmed the uniform morphology of magnetosomes at 200 nm scale bar, (b) HR-TEM image showed the cubo-octahedral shape of magnetosomes at 5 nm scale bar, (c) EDS showed the presence of iron, carbon and oxygen in magnetosome

2.6 Extraction of LLO from *L. monocytogenes* and detection using magnetosomes–antibody complex

Overnight culture of *L. monocytogenes* (MTCC-657) was selected and inoculated in pasteurised milk and water sample. The samples were then incubated at 37°C for 24 h at 120 rpm in an orbital shaker. Once the proper growth was achieved in each sample, they were collected and homogenised for 10 min. The content was centrifuged at 1000 × *g* for 10 min and the LLO protein was separated out from the solid food and cell debris. The extracted LLO protein from each sample was loaded into the wells and ELISA was performed using magnetosomes (2 mg/ml)–anti-LLO antibody (0.5 µg/ml) complex.

The extracted LLO protein was also detected in EIS [43]. The protein and the magnetosomes (2 mg/ml)–anti-LLO antibody (0.5 µg/ml) complex (1:1) were added in a tube. The content was mixed properly by continuously rocking the tube at 37°C for 30 min. The magnetosomes–anti-LLO antibody–LLO protein complex was separated out using an external magnetic field and 10 µl of it was placed on the electrode for EIS measurements. The specificity of the magnetosomes–anti-LLO antibody complex was verified in EIS using three other pathogens (*S. typhimurium*, *E. coli* and *S. aureus*).

The proteins were extracted from these pathogens and compared with the previously extracted LLO protein. The detection was done using magnetosomes (2 mg/ml)–anti-LLO antibody (0.5 µg/ml) complex.

2.7 Detection of *L. monocytogenes* in water and milk sample

The overnight culture of *L. monocytogenes* was centrifuged (1000 × *g*, 5 min), washed and resuspended in PBS buffer to maintain 10⁷ Cfu/ml concentrations. Milk and water samples were collected, subsequently 100 µl of *L. monocytogenes* (10⁷ Cfu/ml) was added to 900 µl of each sample. The milk and water samples were serially diluted till 10¹ Cfu/ml concentration. The sensitivity and capture efficiency of the sensor was verified using protocols modified from Varshney and Li [44]; Setterington and Alocilja [45]. Briefly, 100 µl of magnetosomes (2 mg/ml)–anti-LLO antibody (0.5 µg/ml) complex was added to 100 µl of each set contaminated by *L. monocytogenes* (10¹–10⁷ Cfu/ml in milk/water). The solutions were mixed uniformly in an orbital shaker at 37°C for 30 min. The magnetosomes–anti-LLO antibody–*L. monocytogenes* complex was separated out from the rest of the solution using a bar magnet and washed twice with distilled water. The impedance was measured by placing 10 µl of the complex on the SPCE. The capture efficiency of the magnetosomes–anti-LLO antibody complex was performed [46]. The magnetosomes–anti-LLO antibody–*L. monocytogenes* complex from each set of test sample (10¹–10⁷ Cfu/ml in milk/water) was plated on Brain Heart Infusion Agar. A series of control set containing *L. monocytogenes* (10¹–10⁷ Cfu/ml) in milk/water sample were also plated in the selective media (see (1)). The FESEM analysis for the interaction of *L. monocytogenes* with magnetosome–anti-LLO antibody complex was also carried out. The complex was collected from the tube (10³ in water) and briefly placed on silica plate. Then, 0.25% glutaraldehyde was added on the complex and left for overnight incubation at 4°C. Once incubation was over, a magnet was attached below the plate. Then continuous dehydration of cells in a grade series was carried out using ethanol (70, 80, 90 and 100%). The cells were then viewed under the microscope.

3 Results

3.1 Extraction and analytical characterisation of magnetosomes

Magnetosomes were extracted from *Magnetospirillum sp.* RJS-1. There was a total of 4–6 mg/l yield of magnetosomes. The FESEM analysis confirms the size of magnetosomes (33–62 nm) in nano-range (Fig. 1a). HR-TEM analysis revealed the cubo-octahedral shape and uniform size distribution of magnetosome (Fig. 1b). EDS confirmed the presence of iron in magnetosomes along with carbon and oxygen. Fe–O bond present in Fe₃O₄ shows the magnetic nature of magnetosomes (Fig. 1c).

3.2 Binding of magnetosomes with anti-LLO antibody

The conjugation of anti-LLO antibody with magnetosomes was confirmed by the difference in the absorbance. The average absorbance of magnetosomes (1 mg/ml)–anti-LLO antibody complex (0.232) was higher as compared to the absorbance of only magnetosomes (0.171) and the absorbance of only anti-LLO antibody (0.122) (Fig. 2a). Similarly, the average absorbance of magnetosomes (2 mg/ml)–anti-LLO antibody (0.256) was higher than the absorbance of the components alone (magnetosomes 0.19 and anti-LLO antibody 0.122) (Fig. 2b).

EIS analyses the interfacial electron transfer to determine charge transfer resistance (R_{CT}) at the modified electrode surface. The Nyquist plot was obtained for real (Z_{re}) versus imaginary (Z_{im}). The impedance of bare SPCE showed slight resistance to

$$\text{Capture efficiency} = \frac{\text{(Number of viable cells captured)}}{\text{(Number of viable cells in an original dilution)}} \times 100 \quad (1)$$

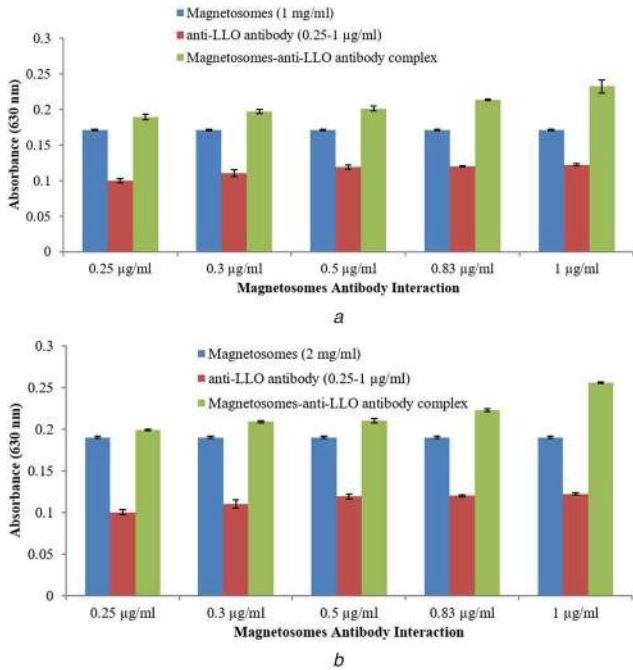


Fig. 2 Interaction of anti-LLO antibody at various concentrations (0.25–1 µg/ml) with magnetosomes (a) 1 mg/ml, (b) 2 mg/ml

Table 1 Interaction of magnetosomes with anti-LLO antibody

Electrode surface	R_S , Ω	C_{dl} , μF	R_{CT} , Ω
bare	181	1.44	685
Ab	190	2.15	1064
magnetosomes	186	2.56	1208
magnetosomes–Ab	192	2.97	2762

R_S : solution resistance, C_{dl} : double layer capacitance, R_{CT} : charge transfer resistance.

Table 2 Various concentrations (0.25–1 µg/ml) of anti-LLO antibody (Ab)

Concentration of Ab	R_S , Ω	C_{dl} , μF	R_{CT} , Ω
bare	117	1.54	423
0.25 µg/ml	105	1.65	996
0.3 µg/ml	115	1.86	1058
0.5 µg/ml	104	2.07	1189
0.8 µg/ml	121	2.22	1419
1 µg/ml	106	2.57	1556

electrolyte with R_{CT} 685 Ω . Subsequently, when anti-LLO antibody (0.5 µg/ml) was applied to the electrode, a slight increase in resistance (R_{CT} = 1064 Ω) was observed. The presence of magnetosomes (2 mg/ml) on the surface of electrode also exerted resistance (R_{CT} = 1208 Ω) to the electrolyte. However, magnetosomes (2 mg/ml)–anti-LLO antibody (0.5 µg/ml) complex exhibited good resistance (R_{CT} = 2762 Ω) compared to magnetosomes and anti-LLO antibody, displaying a successful binding between magnetosomes and anti-LLO antibody (Fig. 3a, Table 1).

Further, the various concentrations of anti-LLO antibody (0.25–1 µg/ml) and its interaction with the magnetosomes were also studied in EIS. The lowest concentration of anti-LLO antibody (0.25 µg/ml) expressed R_{CT} of 996 Ω . Once the concentration of antibody (0.3 µg/ml) was increased, increase in resistance (R_{CT} = 1058 Ω) was observed, followed by 1189 Ω at 0.5 µg/ml, 1419 Ω at 0.83 µg/ml and 1556 Ω at 1 µg/ml. The calibration graph also displayed regression coefficient (R^2 value) of 0.9918 depicting linearity between concentration and R_{CT} (Fig. 3b, Table 2).

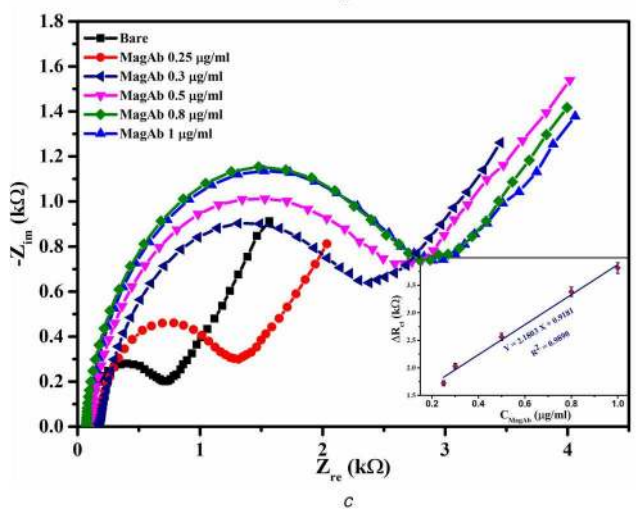
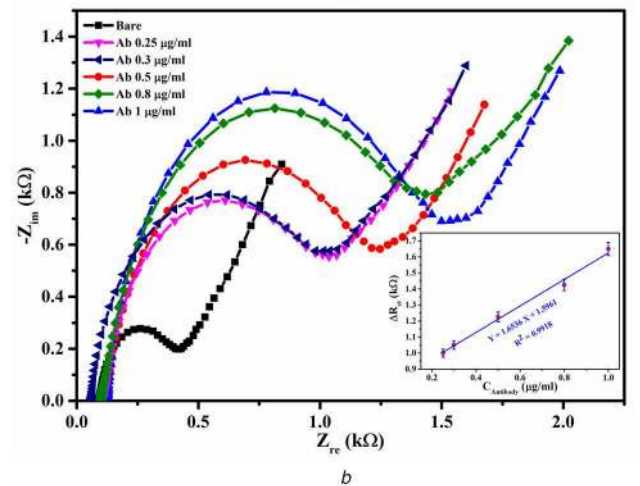
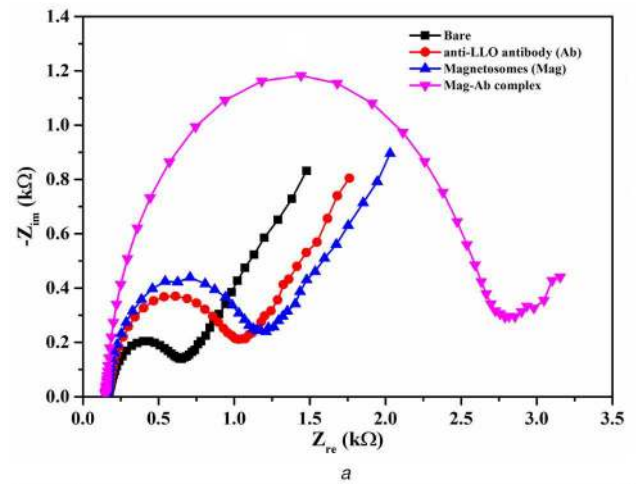


Fig. 3 Nyquist diagrams and the corresponding simulated results (solid line) of SPCEs obtained under the following conditions

(a) Interaction of magnetosomes with anti-LLO antibody, (b) Resistance for various concentration of anti-LLO antibody (0.25–1 µg/ml), (c) Resistance for various concentration of magnetosomes–anti-LLO antibody (0.25–1 µg/ml) complex

Similarly, interaction of magnetosomes with various concentrations of anti-LLO antibody (0.25–1 µg/ml) exerted change in resistance. The interfacial charge transfer resistance also increased with the rise in concentration of antibody in magnetosomes–antibody complex (1314 Ω at 0.25 µg/ml, 2392 Ω at 0.3 µg/ml, 2682 Ω at 0.5 µg/ml, 3295 Ω at 0.83 µg/ml and 3754 Ω at 1 µg/ml). The calibration graph for magnetosomes (2 mg/ml)–anti-LLO antibody (0.25–1 µg/ml) complex showed linearity (R^2 value = 0.9890; Fig. 3c, Table 3).

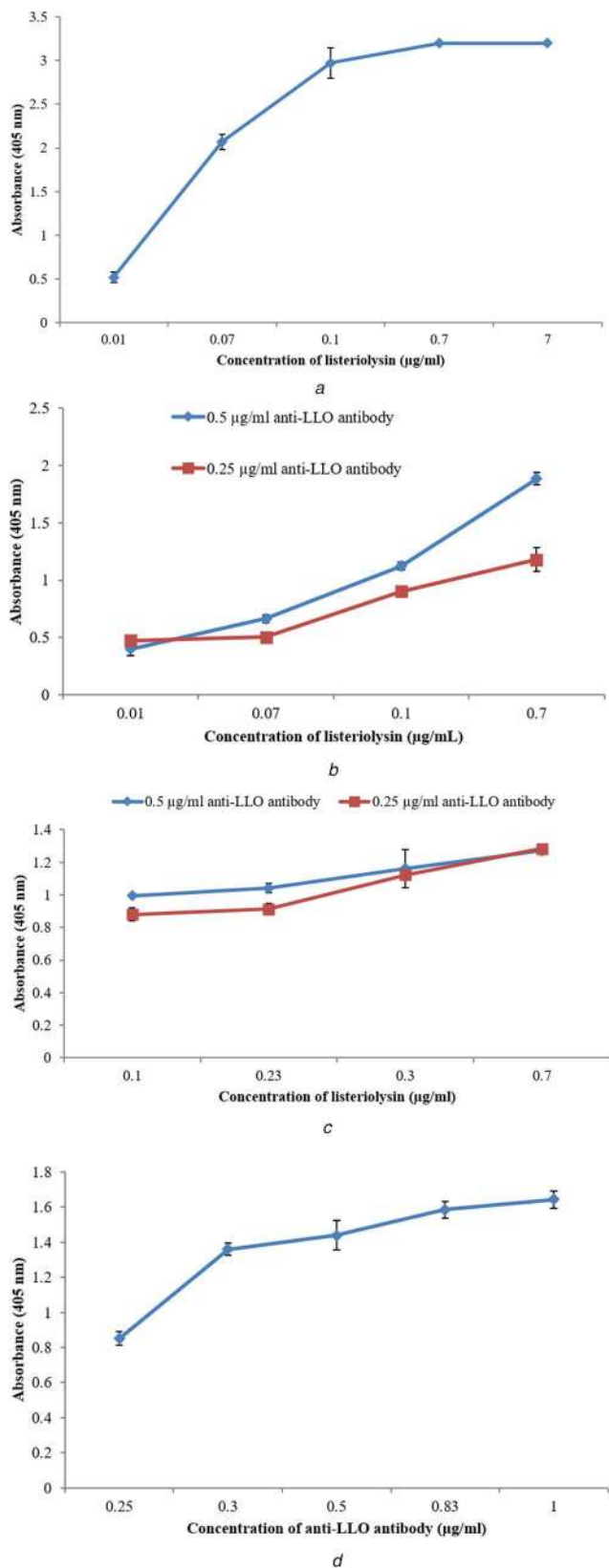


Fig. 4 Absorption spectra for immunoassay to colorimetrically standardise LLO concentration (0.01–7 µg/ml) (a) At 1 µg/ml anti-LLO antibody, (b) Using two concentrations (0.5 µg/ml, 0.25 µg/ml) of anti-LLO antibody, (c) Listeriolysin concentration (0.1–7 µg/ml) using anti-LLO antibody (0.5 µg/ml, 0.25 µg/ml), (d) Standardise anti-LLO antibody concentration (0.25–1 µg/ml) using secondary antibody-HRP (1 µg/ml)

3.3 Screening of LLO from *L. monocytogenes*

3.3.1 Screening of LLO without magnetosome: Various concentrations of LLO (0.01–7 µg/ml) were optimised in ELISA. Anti-LLO antibody (0.25–1 µg/ml) and secondary antibody-HRP

Table 3 Various concentrations (0.25–1 µg/ml) of magnetosomes–anti-LLO antibody (MagAb)

Concentration of MagAb	R_S , Ω	C_{dl} , μF	R_{CT} , Ω
bare	118	1.45	580
0.25 µg/ml	115	2.01	1314
0.3 µg/ml	105	2.48	2392
0.5 µg/ml	114	2.97	2682
0.8 µg/ml	101	3.25	3295
1 µg/ml	107	3.92	3754

(1 µg/ml) was used in the assay. Among the different concentration, 0.01 µg/ml concentration of LLO, 0.5 µg/ml concentration of anti-LLO antibody and 1 µg/ml concentration of secondary antibody-HRP (Figs. 4a–d) were selected as standard concentration for the assay.

3.3.2 Binding of magnetosomes–anti-LLO antibody complex with LLO: Further, the interaction of magnetosomes–anti-LLO antibody complex with LLO (0.1 µg/ml) was studied in spectroscopy. The average absorbance of magnetosomes (1 mg/ml)–anti-LLO antibody (1 µg/ml)–LLO complex was observed to be 0.264. The absorbance of magnetosomes–antibody–LLO complex was comparatively higher than the absorbance of magnetosomes–anti-LLO antibody complex (0.232) and LLO alone (0.045; Fig. 5a). Similarly, the average absorbance of magnetosomes (2 mg/ml)–anti-LLO antibody–LLO complex (0.284) was higher than only magnetosomes–anti-LLO antibody complex (0.256) and LLO (0.045) (Fig. 5b). Other concentrations of magnetosomes–anti-LLO antibody complex also showed the similar difference in absorbance which indicates the active interaction of LLO with magnetosomes–anti-LLO antibody complex.

3.3.3 ELISA to detect LLO using magnetosome–anti-LLO antibody complex: Magnetosomes were used in two different concentrations (1 and 2 mg/ml) for the assay. Magnetosomes (2 mg/ml)–anti-LLO antibody complex (0.25–1 µg/ml) showed higher absorbance than magnetosomes (1 mg/ml)–anti-LLO antibody complex (0.25–1 µg/ml) and only anti-LLO antibody (0.25–1 µg/ml) (Fig. 6a). Further, LLO (0.1 µg/ml) was detected using magnetosomes (2 mg/ml)–anti-LLO antibody (0.25 µg/ml) complex. A marked difference in absorbance (0.390) was observed between magnetosomes (2 mg/ml)–anti-LLO antibody complex (0.25 µg/ml) and uncoupled anti-LLO antibody (0.25 µg/ml). There was ~25% decrease in usage of anti-LLO antibody when magnetosomes conjugated antibodies were used. 1 mg/ml magnetosomes–anti-LLO antibody complex at 0.25 µg/ml concentration showed a higher absorbance (0.990) compared to (0.821) absorbance of uncoupled anti-LLO antibody (0.25 µg/ml; Fig. 6a).

The minimum concentration of LLO was also determined in ELISA. Among the various concentrations (0.01–7 µg/ml) of LLO, 0.01 µg/ml concentration of LLO was detected. The 2 mg/ml of magnetosomes coupled with anti-LLO antibody (0.25 µg/ml) showed similar absorbance (0.496) to the only antibody (0.25 µg/ml) (0.492) in order to detect the LLO (Fig. 6b). This signifies successful detection of LLO using magnetosomes coupled antibody.

3.3.4 Detection of LLO in SPCE: The bare SPCE exhibited a small semicircle at high-frequency region and a straight line at low-frequency region expressing a Warburg resistance. The presence of Warburg signifies a diffusion-controlled process with R_{CT} 707 Ω . The electrode modified with anti-LLO antibody showed R_{CT} value of 1193 Ω , depicting twofold increase in resistance. This suggests the electron transfer process by charge transfer rather than diffusion. Similarly, when various concentrations of LLO (0.01–7 µg/ml) were interacted with anti-LLO antibody on the electrode, variation in the R_{CT} value was evident. The subsequent increase in the concentration of LLO

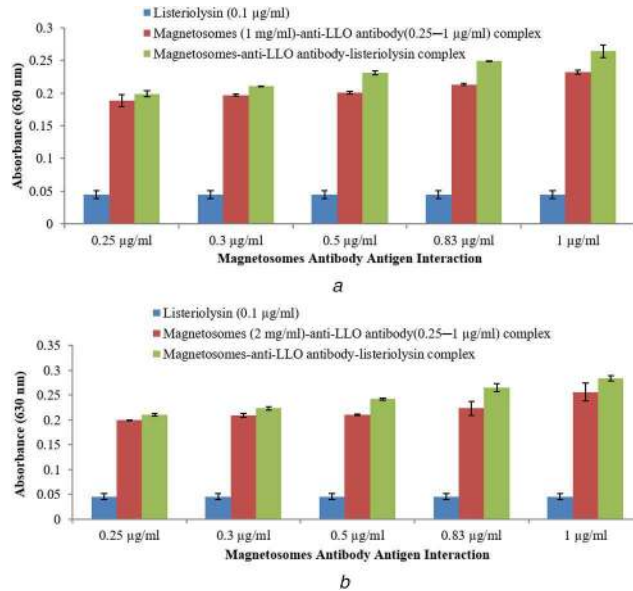


Fig. 5 Interaction of LLO (0.1 µg/ml) with (a) Magnetosomes (1 mg/ml)-anti-LLO antibody (0.25-1 µg/ml) complex, (b) Magnetosomes (2 mg/ml)-anti-LLO antibody (0.25-1 µg/ml) complex

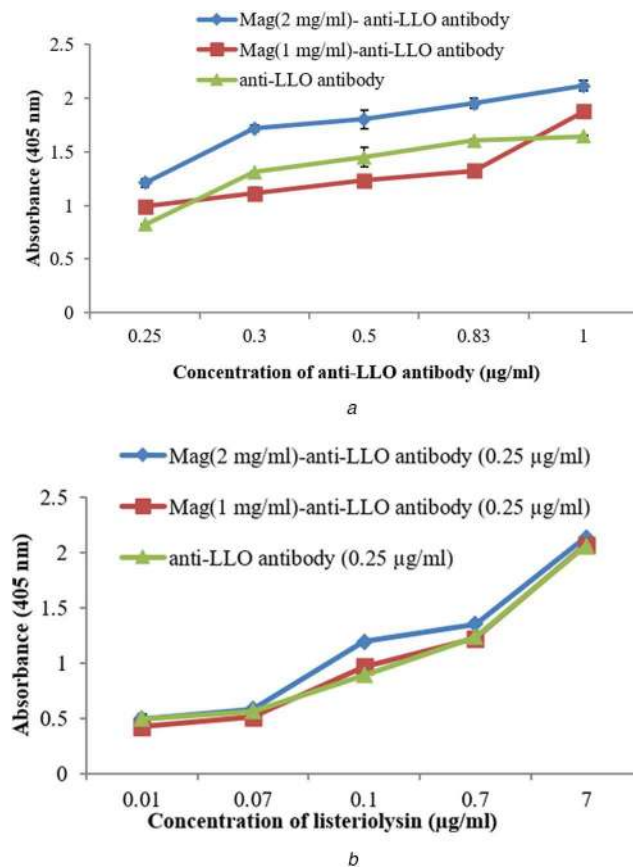
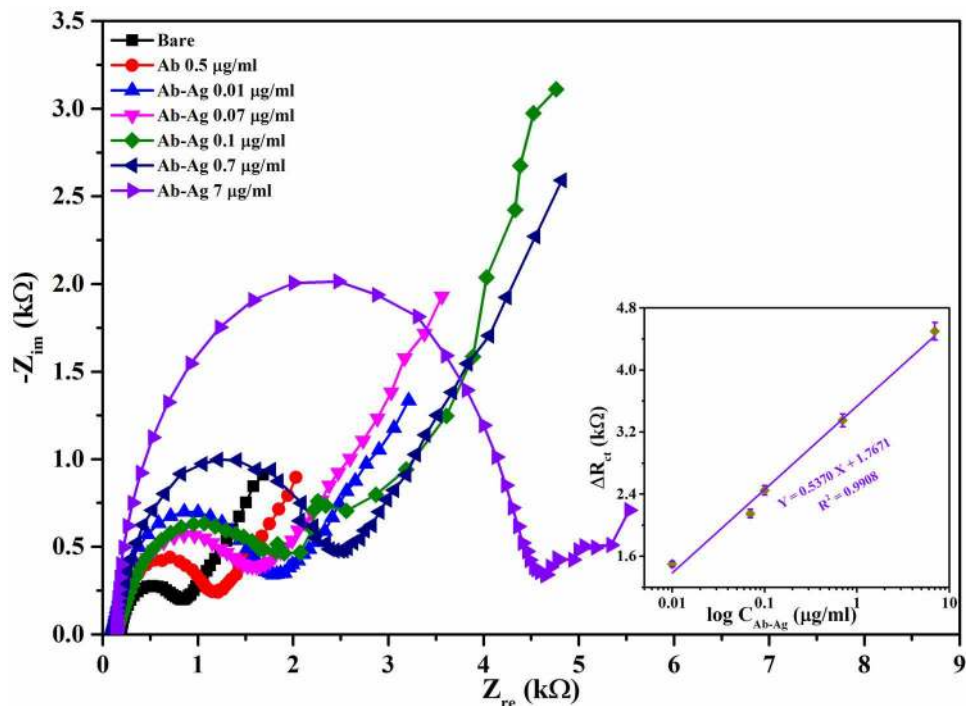


Fig. 6 Absorption spectra for immunoassay to colorimetrically compare the absorbance of (a) Magnetosomes (2 mg/ml)-anti-LLO antibody complex, magnetosomes (1 mg/ml)-anti-LLO antibody complex and uncoupled LLO antibody from 0.25 µg/ml to 1 µg/ml concentration range, (b) Magnetosomes (2 mg/ml)-anti-LLO antibody (0.25 µg/ml) complex, magnetosomes (1 mg/ml)-anti-LLO antibody (0.25 µg/ml) complex and uncoupled LLO antibody (0.25 µg/ml) to detect LLO (0.01-7 µg/ml)

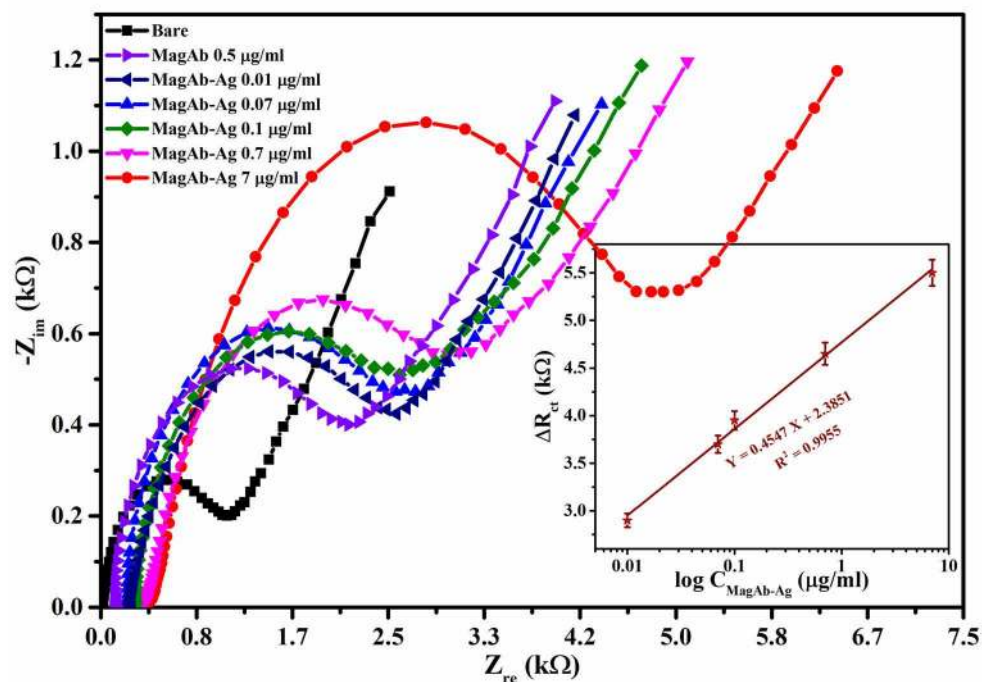
showed elevation in R_{CT} value (0.01 µg/ml = 1599 Ω; 0.07 µg/ml = 1845 Ω; 0.1 µg/ml = 2070 Ω; 0.7 µg/ml = 2519 Ω; 7 µg/ml = 4510 Ω, Fig. 7a, Table 4). LLO interaction with magnetosomes-anti-LLO antibody was also studied in EIS. The magnetosomes-anti-LLO antibody (0.5 µg/ml) showed an R_{CT} value of 2564 Ω.

The further interaction of LLO with magnetosomes-anti-LLO antibody (0.5 µg/ml) showed higher R_{CT} value compared to magnetosomes-antibody complex. The various R_{CT} with different concentration of LLO are as follows (3064 Ω at 0.01 µg/ml; 3283

Ω at 0.07 µg/ml; 3575 Ω at 0.1 µg/ml; 3820 Ω at 0.7 µg/ml; 5554 Ω at 7 µg/ml, Fig. 7b, Table 5). The calibration graph showed the linearity in relationship between LLO concentration and resistance produced in both set (antibody alone = R^2 value 9918; magnetosomes-antibody complex = R^2 value 9955). The electron transfer on the electrode surface was controlled through charge transfer rather than diffusion.



a



b

Fig. 7 Nyquist diagrams and the corresponding simulated results (solid line) of SPCEs obtained under the following conditions

(a) Interaction of anti-LLO antibody (0.5 µg/ml) with LLO at various concentrations (0.01–7 µg/ml), (b) Interaction of magnetosomes (2 mg/ml)–anti-LLO antibody (0.5 µg/ml) complex with LLO at various concentrations (0.01–7 µg/ml)

Table 4 Anti-LLO antibody (Ab) interacting with different concentrations (0.01–7 µg/ml) of LLO (Ag)

Concentration of Ab–Ag	R_S , Ω	C_{dl} , μF	R_{CT} , Ω
bare	116	1.34	707
Ab 0.5 µg/ml	108	1.76	1193
Ab–Ag (0.01 µg/ml)	125	1.95	1599
Ab–Ag (0.07 µg/ml)	105	2.06	1845
Ab–Ag (0.1 µg/ml)	114	2.47	2070
Ab–Ag (0.7 µg/ml)	101	2.92	2519
Ab–Ag (7 µg/ml)	108	3.17	4510

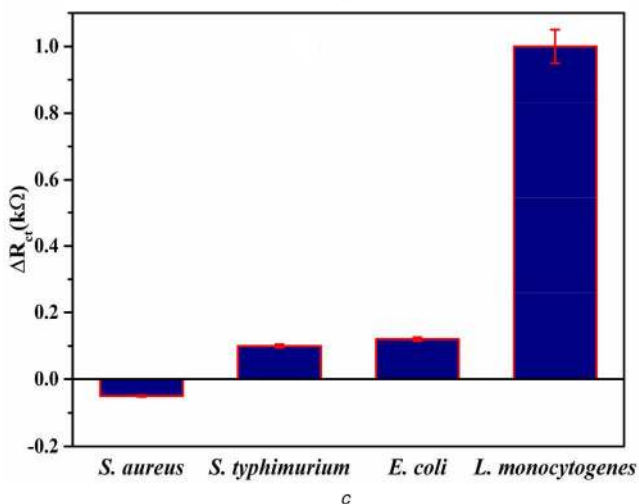
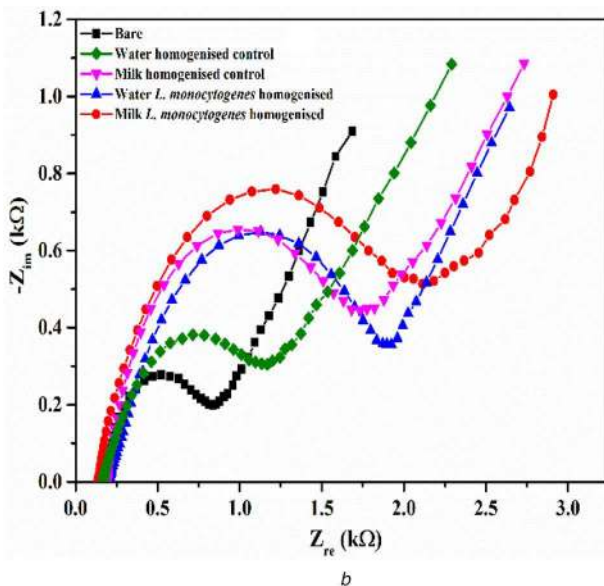
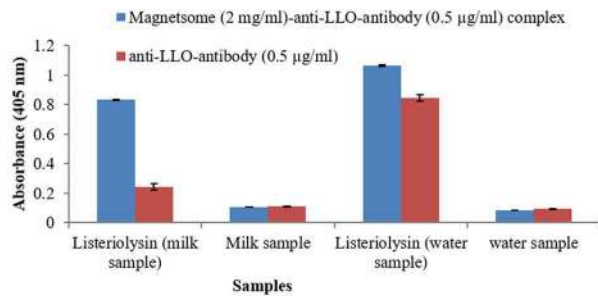
R_S : solution resistance, C_{dl} : double layer capacitance, R_{CT} : charge transfer resistance.

3.4 LLO detection in contaminated sample through ELISA and EIS

The LLO extracted from milk and water sample was verified in ELISA. Among both the samples, LLO was more evidently extracted from the contaminated water sample. The optical density was also higher in water sample showing 1.064 and 0.845 for magnetosomes–antibody complex and only antibody, respectively. In case of milk sample, the absorbance was 0.832 for magnetosomes–antibody complex and 0.244 for antibody alone. The uninfected milk and water sample showed absence of LLO (Fig. 8a). The magnetosomes (2 mg/ml)–anti-LLO antibody (0.5 µg/ml) complex could efficiently detect the LLO in homogenised food sample.

Table 5 Magnetosomes–anti-LLO antibody (Mag-Ab) interacting with different concentrations (0.01–7 µg/ml) of LLO (Ag)

Conc. of MagAb–Ag	R_S , Ω	C_{dl} , μF	R_{CT} , Ω
bare	116	1.75	854
MagAb 0.5 µg/ml	107	1.97	2564
MagAb–Ag (0.01 µg/ml)	95	2.25	3064
MagAb–Ag (0.07 µg/ml)	115	2.86	3283
MagAb–Ag (0.1 µg/ml)	94	3.07	3575
MagAb–Ag (0.7 µg/ml)	121	3.72	3820
MagAb–Ag (7 µg/ml)	109	4.07	5554

**Fig. 8** Assays for LLO detection

(a) ELISA, (b) EIS to detect LLO extracted from homogenised milk and water sample, (c) Cross-reactivity assay

The LLO extracted from contaminated samples was also tested on SPCE's using magnetosomes (2 mg/ml)–anti-LLO antibody (0.5 µg/ml) complex. The R_{CT} values for the contaminated samples

Table 6 Various modifications on SPCE with LLO extracted from contaminated water and milk sample

Electrode surface	R_S , Ω	C_{dl} , μF	R_{CT} , Ω
bare	180	1.44	825
water homogenised control	192	2.15	1164
milk homogenised control	187	2.56	1692
water <i>L. monocytogenes</i> homogenised	194	2.97	1870
milk <i>L. monocytogenes</i> homogenised	185	3.12	2146

were 2146 Ω (milk) and 1870 Ω (water), respectively. There was approximately two-fold increase in resistance when compared with the corresponding controls (milk = 1692 Ω ; water = 1164 Ω) shown in Fig. 8b, Table 6.

The magnetosomes (2 mg/ml)–anti-LLO antibody (0.5 µg/ml) complex developed in this study had been tested for selective determination of *L. monocytogenes* by comparing its functioning with negative samples such as *S. typhimurium*, *E. coli* and *S. aureus*. Cross-reactivity experiments were performed with various proteins extracted from other food pathogens and the results are displayed in Fig. 8c. From the computed charge transfer resistance R_{CT} , it is evident that our antibody specifically interacts with *L. monocytogenes*, thereby providing insignificant response with other proteins and proving its selective sensing of the targeted species. The developed or fabricated sensor was highly specific to LLO.

3.5 Sensing of *L. monocytogenes* by magnetosomes-based biosensor in food sample

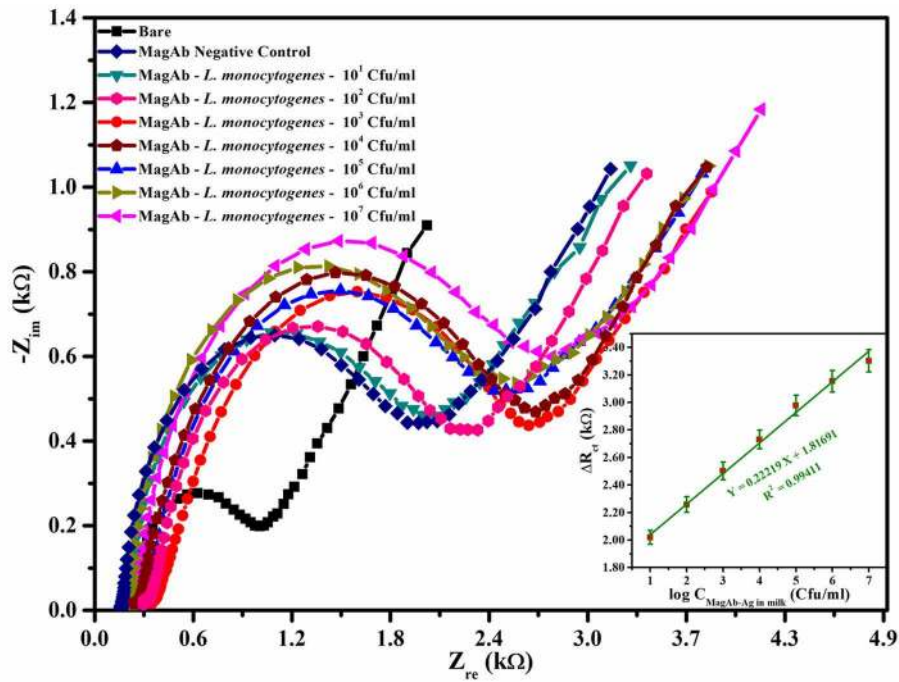
The magnetosomes (2 mg/ml)–anti-LLO antibody (0.5 µg/ml) complex was used to directly detect the *L. monocytogenes* in food sample. The detection limit was 10^1 CfU/ml in milk and water for the developed sensor. The R_{CT} values in water were obtained as follows 1868, 2229, 2420, 2709, 2987, 3145, 3293 Ω at ten-fold dilutions from 10^1 to 10^7 CfU/ml, respectively (Fig. 9a, Table 7). Similarly, the R_{CT} values in milk were also obtained as 1986, 2092, 2102, 2490, 2878, 3154 and 3393 Ω with increase in number of *L. monocytogenes* (Fig. 9b, Table 8).

There was liner relationship between concentration of *L. monocytogenes* in food sample and R_{CT} value (milk = 0.9933; water = 0.9936; Figs. 9a and b). The capture efficiency confirmed positive interaction of Listeria cells with magnetosomes–antibody complex. The electron transfer process is controlled by charge transfer rather than diffusion.

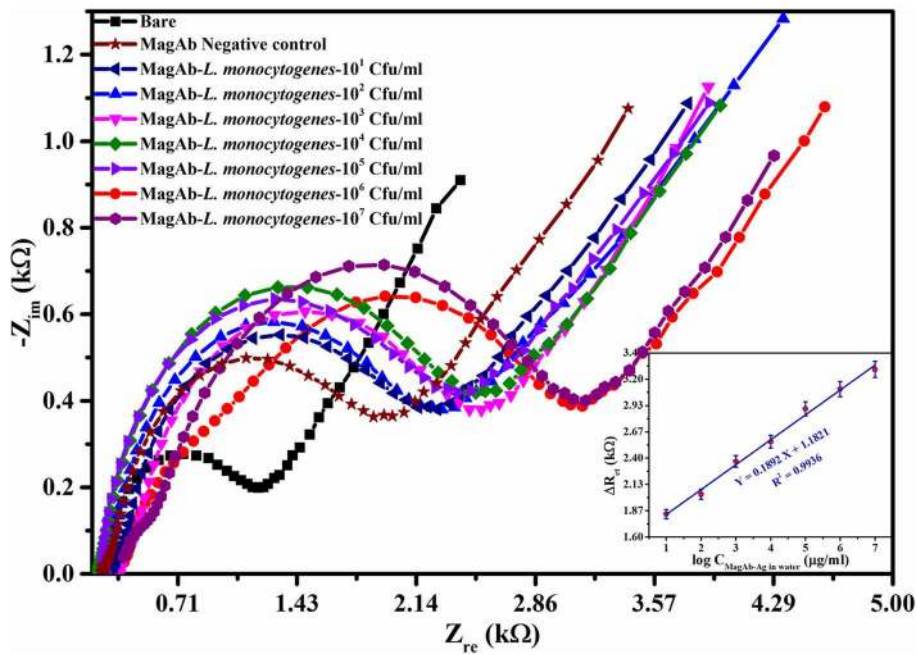
FESEM analysis confirmed the positive interaction of magnetosome–anti-LLO antibody complex with *L. monocytogenes*. The cubo-octahedral shaped magnetosome was seen enclosed around the rod-shaped *L. monocytogenes* (Fig. 9c).

4 Discussion

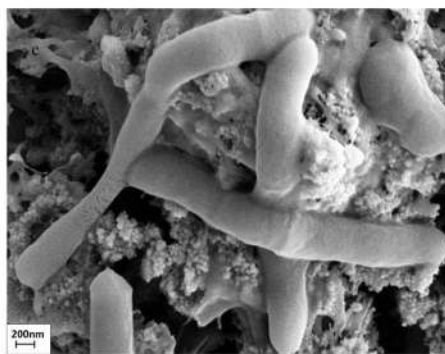
The recent advancements in biotechnology pays way for commercialised application of magnetosomes but, the lack of focus has left the area unexplored. We mainly concentrate on designing magnetosomes-based biosensors to detect the *L. monocytogenes* in food sample in a cost-effective, sensitive and rapid manner. Our study focuses on magnetosomes which are extracted from novel strain *Magnetospirillum sp.* RJS-1 [38]. The novel strain



a



b



c

Fig. 9 Nyquist diagrams and the corresponding simulated results (solid line) of SPCEs obtained under the interaction of magnetosome–LLO antibody complex with various concentrations of *L. monocytogenes* in (a) Milk sample, (b) Water sample, (c) FESEM analysis of magnetosome–anti-LLO antibody complex conjugating with *L. monocytogenes*

Table 7 Fitting parameters for various modifications on SPCE with different concentrations of *L.monocytogenes* in milk sample

Conc. of <i>L. monocytogenes</i> in milk	R_S, Ω	$C_{dl}, \mu F$	R_{CT}, Ω
bare	285	1.36	1050
negative	284	1.54	1805
10^1 Cfu/ml	275	2.05	1986
10^2 Cfu/ml	295	2.46	2092
10^3 Cfu/ml	284	2.87	2102
10^4 Cfu/ml	291	3.02	2490
10^5 Cfu/ml	286	3.57	2878
10^6 Cfu/ml	292	3.75	3154
10^7 Cfu/ml	290	3.99	3393

Magnetospirillum sp. RJS-1 shows comparatively better magnetosomes yield (4–6) mg/l than other reported strains AMB-1 and MS-1 [47]. Magnetosomes are synthesised through biomineralisation, possess higher physical and chemical properties than nanoparticles [48]. The magnetic nature of magnetosomes plays a crucial role which can act as a potential tool for the diagnostic and therapeutic purpose [49]. Though, current advance in biotechnology has paid much attention on nanoparticles. Nanoparticles are incapable of direct binding with proteins [50] thereby implementing the use of wide range of linker molecules namely biotin, streptavidin, glutaraldehyde for the conjugation [51–53].

Our study overcomes these drawbacks and presents the direct binding of the anti-LLO antibody with magnetosomes. The magnetosomes possess superior properties that increase the possibility of binding with antibodies [54]. The LLO specific antibody was conjugated with magnetosomes and confirmed through spectroscopic analysis. The direct binding of antibodies with magnetosomes eliminates the problem of affecting the binding kinetics and affinities of biomolecules. LLO was also directly bound to magnetosome–anti-LLO antibody complex and confirmed through spectroscopic analysis. The difference in absorbance and resistance confirmed the conjugation of magnetosomes–anti-LLO antibody complex with LLO. The recent advancements in ELISA depict its use in clinical diagnosis of pathogen [55]. The sensitivity and minute detection limit of traditional ELISA has always been effective for studying the antigen–antibody interaction. ELISA was performed using secondary antibody-HRP to optimise the concentration of magnetosomes–anti-LLO antibody complex and LLO. The use of magnetosomes–anti-LLO antibody complex instead of only anti-LLO antibody widely reduced the concentration of antibody by 25%. Previous reports also presented better functioning of antibodies when used with gold nanoparticles in ELISA [56]. It was also reported that the antibodies when immobilised on magnetosomes, have greater activities [57].

Some reports implement high concentrations of antibodies for conjugation with nanoparticle. Davis *et al.* [27] in 2013 reported that $10 \mu\text{g/ml}$ of anti-listeria antibody was used for coupling with gold nanoparticles for conjugation purpose. Similarly, Wang *et al.* [58] used $10 \mu\text{g/ml}$ of biotinylated anti-*Listeria* antibody along with range of linker molecules to conjugate with gold nanoparticles. Previous studies have reported an immunogenic nanoparticle-based ELISA where $100 \mu\text{g/ml}$ of anti-*L. monocytogenes* antibody was used with gold nanoparticle [59]. However in our study, we comparatively used less concentration of antibody ($0.25 \mu\text{g/ml}$) bound to magnetosomes for detection of LLO in ELISA. In addition, the minimum concentration of LLO necessary for the ELISA was $0.01 \mu\text{g/ml}$.

ELISA assay was preliminary implemented for detection of LLO in laboratory setting. In order to explore the commercial application of our study, we proposed the fabrication of magnetosome-based sensors. For developing a magnetosomes-based biosensors, the magnetosomes–anti-LLO antibody complex was directly coated on SPCE. The magnetic property of

Table 8 Fitting parameters for various modifications on SPCE with different concentrations of *L. monocytogenes* in water sample

Conc. of <i>L. monocytogenes</i> in water	R_S, Ω	$C_{dl}, \mu F$	R_{CT}, Ω
bare	284	1.16	987
negative	286	1.34	1705
10^1 Cfu/ml	285	1.89	1868
10^2 Cfu/ml	295	2.16	2229
10^3 Cfu/ml	284	2.52	2420
10^4 Cfu/ml	291	2.89	2709
10^5 Cfu/ml	298	3.12	2987
10^6 Cfu/ml	296	3.46	3145
10^7 Cfu/ml	291	3.89	3293

magnetosome enables easy immobilisation on the working electrode along with the antibodies using an external magnetic field. This overcomes the drawbacks of indirect immobilisation of antibodies or nanoparticle conjugated antibodies via linkers or chemicals [60]. Additionally, SPCEs are easy to use and are very useful in handling samples like food and human urine [61]. The plastic material present in SPCEs imparts low cost to the product and makes it feasible for one-time use [62]. The various concentrations of magnetosomes–anti-LLO antibody complex were also implemented on SPCEs along with control set of anti-LLO antibody. The R_{CT} values for the control set (antibody only) were comparatively lower in each concentration than the test set (magnetosome conjugated antibody). This confirms better immobilisation of antibodies on SPCEs when used along with magnetosomes. The coated magnetosomes–anti-LLO antibody complex was exposed to various concentrations of LLO. The R_{CT} value confirmed the effective interaction of LLO with magnetosomes–anti-LLO antibody complex. The whole process shows that the electron transferred through the electrode is charge transfer rather than diffusion. Finally, the interaction of LLO with magnetosomes–anti-LLO antibody complex on electrode surface resulted in further increase in R_{CT} value confirming a complete charge transfer with the formation of semicircle to the large range of frequency. The developed sensor was effective in detecting $0.01 \mu\text{g/ml}$ of LLO using magnetosomes–anti-LLO antibody complex.

The magnetosomes-based sensor was then executed on LLO extracted from contaminated milk and water sample. The minimum concentration of magnetosomes (2 mg/ml)–anti-LLO antibody ($0.5 \mu\text{g/ml}$) complex was able to detect the LLO. The presence of LLO in the contaminated milk and water sample was verified in ELISA. Several studies are known to detect LLO from contaminated samples [63–66], however they lack specific detection of the protein in less time. The developed sensor in our study was specific to LLO as it could detect the LLO more effectively compared to other extracted proteins.

Biosensors have been widely used to detect bacterial proteins [22, 67, 68], however direct application of these sensors to samples containing live bacterial cells are limited. In our study, we have directly implemented the developed magnetosomes-based sensor on milk and water sample containing *L. monocytogenes* (10^1 – 10^7 Cfu/ml). The magnetosomes-based sensor was effective in detecting minimum *L. monocytogenes* cell count (10^1 Cfu/ml) manifesting sensitive nature of the sensor. Moreover, the process is rapid and cost effective, as the whole process took total time duration of 30 min with minimum use of buffers. The use of disposable SPCEs also reduces the cost and labour to a large extent. Davis *et al.* [27] developed a gold nanoparticle-modified carbon electrode biosensor where 10^2 Cfu/ml of *L. monocytogenes* was detected from food sample. However, the process was costly as it implemented the use of gold nanoparticles, which was further immobilised on the electrode surface via linker molecules. The capture efficiency also verified the successful interaction of magnetosome–anti-LLO antibody complex with *L. monocytogenes* in our study. The FESEM analysis confirmed the conjugation of

magnetsome–anti-LLO antibody complex with *L. monocytogenes*. This approach could be further advanced in miniature scale for its feasibility in field-based studies which could be easily implemented on medical and industrial scale as well various other sources.

5 Conclusion

The developed biosensor is cost effective, sensitive and specific in detecting LLO protein and *L. monocytogenes*. The process to detect the commercial and extracted protein along with the *Listeria* cells took only 30 min showing rapid nature of the sensor. The sensor was stable throughout the experiment with detection limit of 10¹ Cfu/ml showing proper immobilisation of magnetsome–anti-LLO antibody complex on electrode surface. The developed biosensor can be further miniaturised to develop a portable user-friendly device.

6 Acknowledgment

Our study has been funded in part by a Grant-in-Aid from DBT-No. BT/PR10570/PFN/20/839/2013. SS would like to thank CSIR for providing Senior Research Fellowship.

7 References

[1] Papademas, P., Aspri, M.: 'Dairy pathogens: characteristics and impact', *Dairy Microbiol., Pract. Approach*, 2015, **16**, pp. 69–113

[2] Saha, M., Debnath, C., Pramanik, A.K.: 'Listeria monocytogenes: an emerging food borne pathogen', *Int. J. Curr. Microbiol. App. Sci.*, 2015, **4**, (11), pp. 52–72

[3] DiMaio, H.: 'Listeria infection in women', *Prim. Care. Update. Ob. Gyns.*, 2000, **7**, (1), pp. 40–45

[4] European Food Safety Authority and European Centre for Disease Prevention and Control (EFSA and ECDC): 'The European Union summary report on trends and sources of zoonoses, zoonotic agents and food-borne outbreaks in 2017', *EFSA J.*, 2018, **16**, (12), p. e05500

[5] Martinez-Rios, V., Dalgaard, P.: 'Prevalence of *Listeria monocytogenes* in European cheeses: A systematic review and meta-analysis', *Food Control*, 2018, **84**, pp. 205–214

[6] Basic Information on Emerging Infectious Diseases (EIDs): 'Listeriosis: what we should know'. World Health Organization, Regional Office of South East Asia. Available at http://www.searo.who.int/entity/emerging_diseases/Zoonoses_Listeriosis.pdf?ua=1, accessed September 2019

[7] Selvaganapathi, R., Jeyasekaran, G., Shakila, R.J., et al.: 'Occurrence of *Listeria monocytogenes* on the seafood contact surfaces of Tuticorin Coast of India', *J. Food Sci. Technol.*, 2018, **55**, (7), pp. 2808–2812

[8] Das, S., Lalitha, K.V., Thampran, N., et al.: 'Isolation and characterization of *Listeria monocytogenes* from tropical seafood of Kerala, India', *Ann. Microbiol.*, 2013, **63**, (3), pp. 1093–1098

[9] Belton, B., Bush, S.R., Little, D.C.: 'Not just for the wealthy: rethinking farmed fish consumption in the global south', *Glob. Food Sec.*, 2018, **16**, pp. 85–92

[10] Bhat, S.A., Willayat, M.M., Roy, S.S., et al.: 'Isolation, molecular detection and antibiogram of *Listeria monocytogenes* from human clinical cases and fish of Kashmir, India', *Comp. Clin. Path.*, 2013, **22**, (4), pp. 661–665

[11] Sharma, S., Sharma, V., Dahiya, D.K., et al.: 'Prevalence, virulence potential, and antibiotic susceptibility profile of *Listeria monocytogenes* isolated from bovine raw milk samples obtained from Rajasthan, India', *Foodborne Pathog. Dis.*, 2017, **14**, (3), pp. 132–140

[12] Sarangi, L.N., Panda, H.K., Priyadarshini, A., et al.: 'Prevalence of *Listeria* species in milk samples of cattle of Odisha', *Indian J. Comp. Microbiol. Immunol. Infect. Dis.*, 2009, **30**, (2), pp. 135–136

[13] Mary, M.S., Shrinithiviahshini, N.D.: 'Prevalence of *Listeria monocytogenes* in temple milks offered to the devotees as sacred liquid in Tiruchirappalli, Tamilnadu, India', *Food Public Health*, 2013, **3**, (2), pp. 97–99

[14] Vadia, S., Arnett, E., Haghghat, A.C., et al.: 'The pore-forming toxin listeriolysin O mediates a novel entry pathway of *L. monocytogenes* into human hepatocytes', *PLoS Pathog.*, 2011, **7**, (11), p. e1002356

[15] Gedde, M.M., Higgins, D.E., Tilney, L.G., et al.: 'Role of Listeriolysin O in cell-to-cell spread of *Listeria monocytogenes*', *Infect Immun.*, 2000, **68**, (2), pp. 999–1003

[16] Kayal, S., Charbit, A.: 'Listeriolysin O: a key protein of *Listeria monocytogenes* with multiple functions', *FEMS Microbiol. Rev.*, 2006, **30**, (4), pp. 514–529

[17] Hamon, M.A., Ribet, D., Stavru, F., et al.: 'Listeriolysin O: the Swiss army knife of *Listeria*', *Trends Microbiol.*, 2012, **20**, (8), pp. 360–368

[18] Schlech, IIIW.F., Acheson, D.: 'Foodborne listeriosis', *Clin. Infect. Dis.*, 2000, **31**, (3), pp. 770–775

[19] O'Grady, J., Ruttledge, M., Sedano-Balbas, S., et al.: 'Rapid detection of *Listeria monocytogenes* in food using culture enrichment combined with real-time PCR', *Food Microbiol.*, 2009, **26**, (1), pp. 4–7

[20] Kérouanton, A., Marault, M., Petit, L., et al.: 'Evaluation of a multiplex PCR assay as an alternative method for *Listeria monocytogenes* serotyping', *J. Microbiol. Methods*, 2010, **80**, (2), pp. 134–137

[21] Gopalan, A.I., Lee, K.P., Ragupathy, D., et al.: 'An electrochemical glucose biosensor exploiting a polyaniline grafted multiwalled carbon nanotube/perfluorosulfonate ionomer–silica nanocomposite', *Biomaterials*, 2009, **30**, (30), pp. 5999–6005. Available at <https://doi.org/10.1016/j.biomaterials.2009.07.047>

[22] Ohk, S.H., Koo, O.K., Sen, T., et al.: 'Antibody–aptamer functionalized fibre-optic biosensor for specific detection of *Listeria monocytogenes* from food', *J. Appl. Microbiol.*, 2010, **109**, (3), pp. 808–817

[23] Chen, Q., Lin, J., Gan, C., et al.: 'A sensitive impedance biosensor based on immunomagnetic separation and urease catalysis for rapid detection of *Listeria monocytogenes* using an immobilization-free interdigitated array microelectrode', *Biosens. Bioelectron.*, 2015, **74**, pp. 504–511

[24] Liu, H.B., Du, X.J., Zang, Y.X., et al.: 'SERS-based lateral flow strip biosensor for simultaneous detection of *Listeria monocytogenes* and *Salmonella enterica* serotype Enteritidis', *J. Agric. Food Chem.*, 2017, **65**, (47), pp. 10290–10299

[25] Putzbach, W., Ronkainen, N.: 'Immobilization techniques in the fabrication of nanomaterial-based electrochemical biosensors: A review', *Sensors*, 2013, **13**, (4), pp. 4811–4840

[26] Skottrup, P.D., Nicolaisen, M., Justesen, A.F.: 'Towards on-site pathogen detection using antibody-based sensors', *Biosens. Bioelectron.*, 2008, **24**, (3), pp. 339–348

[27] Davis, D., Guo, X., Musavi, L., et al.: 'Gold nanoparticle-modified carbon electrode biosensor for the detection of *Listeria monocytogenes*', *Ind. Biotechnol.*, 2013, **9**, (1), pp. 31–36

[28] Yang, Z., Zong, X., Ye, Z., et al.: 'The application of complex multiple forklite ZnO nanostructures to rapid and ultrahigh sensitive hydrogen peroxide biosensors', *Biomaterials*, 2010, **31**, (29), pp. 7534–7541. Available at <https://doi.org/10.1016/j.biomaterials.2010.06.019>

[29] Wang, D., Chen, Q., Huo, H., et al.: 'Efficient separation and quantitative detection of *Listeria monocytogenes* based on screen-printed interdigitated electrode, urease and magnetic nanoparticles', *Food Control*, 2017, **73**, pp. 555–561

[30] Wang, W., Liu, L., Song, S., et al.: 'Identification and quantification of eight *Listeria monocytogenes* serotypes from *Listeria* spp. Using a gold nanoparticle-based lateral flow assay', *Microchim. Acta*, 2017, **184**, (3), pp. 715–724

[31] Yang, X., Zhou, X., Zhu, M., et al.: 'Sensitive detection of *Listeria monocytogenes* based on highly efficient enrichment with vancomycin-conjugated brush-like magnetic nano-platforms', *Biosens. Bioelectron.*, 2017, **91**, pp. 238–245

[32] Hussain, M.S., Hess, L.K., Gearhart, M.J., et al.: 'In vitro toxicity of nanoparticles in BRL 3A rat liver cells', *Toxicol. In Vitro*, 2005, **19**, pp. 975–983

[33] Matsunaga, T., Sakaguchi, T., Tadakoro, F.: 'Magnetite formation by a magnetic bacterium capable of growing aerobically', *Appl. Microbiol. Biotechnol.*, 1991, **35**, (5), pp. 651–655. Available at <https://doi.org/10.1007/BF00169632>

[34] Wacker, R., Ceyhan, B., Alhorn, P., et al.: 'Magneto immuno-PCR: a novel immunoassay based on biogenic magnetsome nanoparticles', *Biochem. Biophys. Res. Commun.*, 2007, **357**, (2), pp. 391–396

[35] Bazylinski, D.A., Frankel, R.B., Heywood, B.R., et al.: 'Controlled biomineralization of magnetite (Fe (in3) O (in4)) and Greigite (Fe (in3) S (in4)) in a magnetotactic bacterium', *Appl. Environ. Microbiol.*, 1995, **61**, (9), pp. 3232–3239

[36] Gorby, Y.A., Beveridge, T.J., Blakemore, R.P.: 'Characterization of the bacterial magnetsome membrane', *J. Bacteriol.*, 1988, **170**, (2), pp. 834–841

[37] Tien, H.T., Ottova-Leitmannova, A.: 'Membrane biophysics: as viewed from experimental bilayer lipid membranes', vol. 5 (Elsevier, USA., 2000)

[38] Revathy, T., Jacob, J.J., Jayasri, M.A., et al.: 'Isolation and characterization of *Magnetospirillum* from saline lagoon', *World J. Microbiol. Biotechnol.*, 2016, **32**, p. 109

[39] Hungate, R.E.: 'The anaerobic mesophilic cellulolytic bacteria', *Bacteriol. Rev.*, 1950, **14**, (1), p. 1

[40] Alphandery, E., Guyot, F., Chebbi, I.: 'Preparation of chains of magnetosomes, isolated from *Magnetospirillum magneticum* strain AMB-1 magnetotactic bacteria, yielding efficient treatment of tumors using magnetic hyperthermia', *Int. J. Pharm.*, 2012, **434**, (1), pp. 444–452

[41] Woo, M.A., Kim, M.I., Jung, J.H., et al.: 'A novel colorimetric immunoassay utilizing the peroxidase mimicking activity of magnetic nanoparticles', *Int. J. Mol. Sci.*, 2013, **14**, (5), pp. 9999–10014

[42] Wu, H., Zuo, Y., Cui, C., et al.: 'Rapid quantitative detection of brucella melitensis by a label-free impedance immunosensor based on a gold nanoparticle-modified screen-printed carbon electrode', *Sensors*, 2013, **13**, (7), pp. 8551–8563

[43] Varshney, M., Yang, L., Su, X.L., et al.: 'Magnetic nanoparticle-antibody conjugates for the separation of *Escherichia coli* O157: H7 in ground beef', *J. Food Prot.*, 2005, **68**, (9), pp. 1804–1811

[44] Varshney, M., Li, Y.: 'Interdigitated array microelectrode based impedance biosensor coupled with magnetic nanoparticle-antibody conjugates for detection of *Escherichia coli* O157: H7 in food samples', *Biosens. Bioelectron.*, 2007, **22**, (11), pp. 2408–2414

[45] Settingington, E.B., Alcocilja, E.C.: 'Electrochemical biosensor for rapid and sensitive detection of magnetically extracted bacterial pathogens', *Biosensors*, 2012, **2**, (1), pp. 15–31

[46] Sheikhzadeh, E., Chamsaz, M., Turner, A.P.F., et al.: 'Label-free impedimetric biosensor for *Salmonella Typhimurium* detection based on poly [pyrrole-co-3-carboxyl-pyrrole] copolymer supported aptamer', *Biosens. Bioelectron.*, 2016, **80**, pp. 194–200

[47] Heyen, U., Schüller, D.: 'Growth and magnetsome formation by microaerophilic *Magnetospirillum* strains in an oxygen-controlled fermentor', *Appl. Microbiol. Biotechnol.*, 2003, **61**, (5–6), pp. 536–544

- [48] Schüller, D.: 'The biomineralization of magnetosomes in *Magnetospirillum gryphiswaldense*', *Int. Microbiol.*, 2002, **5**, (4), pp. 209–214
- [49] Hergt, R., Hiergeist, R., Zeisberger, M., *et al.*: 'Magnetic properties of bacterial magnetosomes as potential diagnostic and therapeutic tools', *J. Magn. Magn. Mater.*, 2005, **293**, (1), pp. 80–86
- [50] Kocbek, P., Obermajer, N., Cegnar, M., *et al.*: 'Targeting cancer cells using PLGA nanoparticles surface modified with monoclonal antibody', *J. Controlled Release*, 2007, **120**, (1), pp. 18–26
- [51] Hendrickson, W.A., Pähler, A., Smith, J.L., *et al.*: 'Crystal structure of core streptavidin determined from multiwavelength anomalous diffraction of synchrotron radiation', *Proc. Natl. Acad. Sci. U.S.A.*, 1989, **86**, (7), pp. 2190–2194
- [52] Wong, J., Chilkoti, A., Moy, V.T.: 'Direct force measurements of the streptavidin–biotin interaction', *Biomol. Eng.*, 1999, **16**, (1), pp. 45–55
- [53] Amemiya, Y., Tanaka, T., Yoza, B., *et al.*: 'Novel detection system for biomolecules using nano-sized bacterial magnetic particles and magnetic force microscopy', *J. Biotechnol.*, 2005, **120**, (3), pp. 308–314
- [54] Arakaki, A., Nakazawa, H., Nemoto, M., *et al.*: 'Formation of magnetite by bacteria and its application', *J. R. Soc., Interface*, 2008, **5**, (26), pp. 977–999
- [55] Lequin, R.M.: 'Enzyme immunoassay (EIA)/enzyme-linked immunosorbent assay (ELISA)', *Clin. Chem.*, 2005, **51**, (12), pp. 2415–2418
- [56] Ambrosi, A., Airo, F., Merkoçi, A.: 'Enhanced gold nanoparticle based ELISA for a breast cancer biomarker', *Anal. Chem.*, 2009, **82**, (3), pp. 1151–1156
- [57] Nakamura, N., Burgess, G.J., Yagiuda, K., *et al.*: 'Detection and removal of escheria coli using fluorescein isothiocyanate conjugated monoclonal antibody immobilized on bacterial magnetic particles', *Anal. Chem.*, 1993, **65**, pp. 2036–2039
- [58] Wang, H., Li, Y., Slavik, M.: 'Rapid detection of *Listeria monocytogenes* using quantum dots and nanobeads-based optical biosensor', *J. Rapid Meth. Aut. Mic.*, 2007, **15**, (1), pp. 67–76
- [59] Oaew, S., Charlermroj, R., Pattarakankul, T., *et al.*: 'Gold nanoparticles/horseradish peroxidase encapsulated polyelectrolyte nanocapsule for signal amplification in *Listeria monocytogenes* detection', *Biosens. Bioelectron.*, 2012, **34**, (1), pp. 238–243
- [60] Karyakin, A.A., Presnova, G.V., Rubtsova, M.Y., *et al.*: 'Oriented immobilization of antibodies onto the gold surfaces via their native thiol groups', *Anal. Chem.*, 2000, **72**, (16), pp. 3805–3811
- [61] Renedo, O.D., Alonso-Lomillo, M.A., Martínez, M.A.: 'Recent developments in the field of screen-printed electrodes and their related applications', *Talanta*, 2007, **73**, (2), pp. 202–219
- [62] Wang, J., Tian, B., Nascimento, V.B., *et al.*: 'Performance of screen-printed carbon electrodes fabricated from different carbon inks', *Electrochim. Acta*, 1998, **43**, (23), pp. 3459–3465
- [63] Fluit, A.C., Torensma, R., Visser, M.J., *et al.*: 'Detection of *Listeria monocytogenes* in cheese with the magnetic immuno-polymerase chain reaction assay', *Appl. Environ. Microbiol.*, 1993, **59**, (5), pp. 1289–1293
- [64] Rudi, K., Naterstad, K., Drømtorp, S.M., *et al.*: 'Detection of viable and dead *Listeria monocytogenes* on gouda-like cheeses by real-time PCR', *Lett. Appl. Microbiol.*, 2005, **40**, (4), pp. 301–306
- [65] Chen, J., Tang, J., Liu, J., *et al.*: 'Development and evaluation of a multiplex PCR for simultaneous detection of five foodborne pathogens', *J. Appl. Microbiol.*, 2012, **112**, (4), pp. 823–830
- [66] Cheng, N., Xu, Y., Yan, X., *et al.*: 'An advanced visual qualitative and EVA green-based quantitative isothermal amplification method to detect *Listeria Monocytogenes*', *J. Food Saf.*, 2016, **36**, (2), pp. 237–246
- [67] Koubova, V., Brynda, E., Karasova, L., *et al.*: 'Detection of foodborne pathogens using surface plasmon resonance biosensors', *Sens. Actuators B Chem.*, 2001, **74**, (1–3), pp. 100–105
- [68] Alhagail, S., Suaifan, G.A., Zourob, M.: 'Rapid colorimetric sensing platform for the detection of *Listeria monocytogenes* foodborne pathogen', *Biosens. Bioelectron.*, 2016, **86**, pp. 1061–1066